

# Assessment of evolution of loss on ignition matter during heating of iron ores

Vladimir Strezov · Artur Ziolkowski ·  
Tim J. Evans · Peter F. Nelson

Received: 21 April 2009 / Accepted: 29 July 2009 / Published online: 28 August 2009  
© Akadémiai Kiadó, Budapest, Hungary 2009

**Abstract** Ironmaking involves reduction of iron ores to metallic iron using coke, coal or gas as reductants. Although different iron ore reduction processes exist, prior to each reduction type, commonly, the hydroxyl and clay materials present in the iron ores undergo decomposition as a first stage. The mass loss during decomposition of these materials is termed as Loss on Ignition (LOI). The aim of this work is to apply a computer aided thermoanalytical technique to evaluate five different iron ore types during decomposition of the LOI matter and determine associated decomposition temperature ranges and heats of reactions. Fourier Transform Infrared (FTIR) spectroscopy and thermogravimetric analysis (TG) were also incorporated to support the analysis interpretation. Three distinctive temperature ranges of decomposition of iron ore LOI matter were detected. The first region was associated with dehydration of the hygroscopic moisture at a temperature range between 100 and 150 °C. The second region occurred at a temperature range between 260 and 425 °C during which strongly bonded water was released and the OH groups associated with primarily iron oxyhydroxides were fractured. The third range, which occurred at a temperature range of 530 and 605 °C, was related to decomposition of the aluminosilicate clay materials.

**Keywords** Goethite · Hematite · LOI · Iron · Specific heat

## Introduction

Iron and steel production are important industrial processes as iron is the least expensive and most widely used metal in society. The growth rate of annual global production has increased to over 1,300 metric tonnes in 2008 which is more than double compared to steel production in 1970. Pig iron production was approximately 865 Mtpa in 2006 increased to nearly 960 Mtpa in 2008 with steel production of 1,170 Mtpa in 2006 increasing to over 1,360 Mtpa in 2008 [1].

Ironmaking relies upon processes that can convert iron ore to iron and then to steel. To reduce iron ore, oxygen must be removed from the iron. In order to achieve reduction reactions, the iron ore must be heated to high temperatures (>700 °C) under reducing conditions using CO and H<sub>2</sub> as reductants. Typically, these can be produced from coal, coke or natural gas. During heating, the ore particles undergo drying, decomposition and reduction reactions. The thermal removal of bonded water, hydroxyl bonds and other impurities from the iron ore, termed loss on ignition (LOI), affects the efficiency of the conversion process. Each specific type of iron ore has characteristic thermal properties that affect the conversion process and its associated costs.

Understanding the thermal processes involved during release of the LOI matter is important to improve efficiency of the reduction process and to the fundamental understanding of iron ore behaviour with temperature. It is recognised that characterisation of iron ores based on only chemical composition is not sufficient for prediction of the iron ore behaviour during sintering and reduction [2]. The main disadvantage with the current standard tests is that they do not reveal the physical characteristic behaviour of the iron ores with temperature, such as particle strength,

V. Strezov (✉) · A. Ziolkowski · T. J. Evans · P. F. Nelson  
Graduate School of the Environment, Department of  
Environment and Geography, Macquarie University, Sydney,  
NSW 2109, Australia  
e-mail: vstrezov@gse.mq.edu.au

degradation, porosity and swelling. There is an indication that changes in the physical properties of the iron ores are related to the release of volatiles during heating of the ores and during their reduction [3]. Thermal analysis is potentially an additional assessment method that can provide further insight into the thermophysical behaviour of the iron ores with temperature. Previously, thermogravimetric analysis, Differential Thermal Analysis and Differential Scanning Calorimetry were applied to study behaviour of natural and synthetic goethite, hematite, related iron ore types and clay materials [4–11].

A recently developed Computer Aided Thermal Analysis technique [12] offers an opportunity for expanding the current knowledge of thermal assessment of iron ores. In this method two thermocouples are used to measure sample temperatures during heating of samples at continuous heat flux increments, enabling simultaneous estimate of the specific heat and heats of reactions of the heated samples. The work presented here shows thermal assessment of a range of different iron ores using the computer aided thermoanalytical technique combined with Fourier Transform Infrared Analysis and thermogravimetric method in order to accurately determine the apparent specific heat, temperature ranges of the release of the Loss on Ignition matter as well as associated changes in the heats of reactions.

## Experimental

### Materials

Five iron ore samples selected for this study differed in their origin as well as iron ore type. Three of the samples (IO1, IO2 and IO5) were of Australian origin, IO3 was from India, while IO4 was Brazilian iron ore. IO1 sample was close to pure goethite, IO5 close to a pure hematite, while the remaining three samples may be described as goethitic hematite. Prior to analysis, each sample was dried at 110 °C for 2 h, according to the international standard ISO 2596. The chemical composition of iron ores was determined using X-Ray fluorescence (XRF) analysis method in a standard procedure defined by the international ISO 9516 standard. According to this method, the XRF instrument is first calibrated using an XRF calibration standard, which consists of a mixture of 64% Fe<sub>2</sub>O<sub>3</sub>, 9.5% SiO<sub>2</sub>, 4.2913% CaO, 2% Mn<sub>3</sub>O<sub>3</sub>, 5% Al<sub>2</sub>O<sub>3</sub>, 1.5% TiO<sub>2</sub>, 5% MgO, 2.66% P<sub>2</sub>O<sub>5</sub>, 2.3% SO<sub>3</sub> and a range of other minor elements not reported in this work. The calibration standard and iron ore samples are then fused in an alkaline flux consisting of 12 parts Li<sub>2</sub>B<sub>4</sub>O<sub>7</sub> and 22 parts LiBO<sub>2</sub> at a sample to flux ratio of 1:10. The mixture is pressed to form discs which are subjected to X-Ray fluorescence analysis. Standard maximum acceptable deviations for the XRF

**Table 1** Chemical composition of the iron ore samples expressed as mass percent/wt%

	IO1	IO2	IO3	IO4	IO5
Fe <sub>2</sub> O <sub>3</sub>	84.14	90.06	88.85	95.35	98.11
SiO <sub>2</sub>	4.44	2.4	3.37	1.16	0.89
Al <sub>2</sub> O <sub>3</sub>	1.43	1.6	3.48	0.96	0.35
CaO	0.11	0.06	0.06	0.06	0.13
MgO	0.07	0.08	0.08	0.05	0.05
TiO <sub>2</sub>	0.06	0.06	0.11	0.04	0.012
SO <sub>3</sub>	0.027	0.067	0.025	0.02	0.005
Mn <sub>3</sub> O <sub>4</sub>	0.06	0.12	0.12	0.79	0.01
P <sub>2</sub> O <sub>5</sub>	0.11	0.13	0.11	0.06	0.13
LOI <sup>a</sup>	9.53	5.07	3.45	1.41	0.53

<sup>a</sup> Loss on ignition defined as iron ore mass loss measured at 1,000 °C

results are 0.1% for Fe<sub>2</sub>O<sub>3</sub> and 1% for the mass of the remaining elements. Chemical composition of each iron ore sample determined with the XRF analysis is displayed in Table 1.

### Experimental methods

The iron ore samples used in this work were subjected to thermal evaluation to determine their thermal behaviour during heating. Specific heats of the samples were determined using a Computer Aided Thermal Analysis technique. The apparatus consists of an infrared furnace and arrangement of internals for heating of a packed bed of sample. The analysed samples weighing between 5 and 7 g were packed at a density of 3,000–4,000 kg m<sup>-3</sup> in a silica glass tube. The packed samples were insulated on the sides with ceramics and heated under argon atmosphere at a constant flow rate of 5 ml/min. Heating rate of the furnace was fixed at 10 °C min<sup>-1</sup> and heating carried out until the heating element reached 900 °C.

Specific heat of the examined iron ores were estimated simultaneously during continuous heating by applying an inverse numerical technique to the measured temperatures of the heating element and centre and surface temperatures of the sample. For the purpose of these calculations, the sample was divided into a grid with assumed number of nodes across the radius. The heat balance for each node was calculated based on heat conduction principle where heat accumulated by the node equals difference of input and output heats from the node. Estimated specific heat in this case had apparent values. During an endothermic heat effect, the specific heat showed increasing values, while during an exothermic reaction the specific heat values decreased. A more detailed description of the experimental procedure and evaluation technique using various calibration standards can be found elsewhere [12].

A Mettler Toledo thermogravimetric analysis instrument (TGA/DSC 1 Stare System) operated with Stare software was employed to determine mass loss of the samples with temperature. Samples were placed in an alumina cylindrical crucible with an additional empty crucible employed as a reference. All experiments were carried out under nitrogen as a carrier gas flowing at a rate of  $20 \text{ ml min}^{-1}$ , with a heating rate set at  $10 \text{ }^\circ\text{C min}^{-1}$  to match the computer thermal analysis conditions. The buoyancy correction for the TG data was conducted using a blank experiment with no sample placed in both of the alumina crucibles prior to each sample run.

The FT-IR spectra were recorded in Nicolet 6700 FT-IR spectrometer applying Attenuated Total Reflectance (ATR) method with diamond crystal. The total number of scans was 32 with spectral resolution of  $4 \text{ cm}^{-1}$ . Omnic Spectra software was used to analyse the data and assist with interpretation of the FTIR spectra.

## Results

The volumetric specific heat results obtained for the iron ore samples selected for this study are shown in Fig. 1. The

specific heats showed a range of endothermic reactions throughout the heating, mostly associated with removal of water, hydroxyl bonds, decomposition of the clay material bound in the iron ore and the magnetic reaction of hematite. The first three reactions can be associated with the decomposing iron ore matter, also termed as Loss on Ignition. These reactions were further analysed for the temperature range of detected reaction, as well as heats of reactions and mass losses associated with each region, as presented in Table 2. The heats of reactions were estimated by subtracting the integral of the measured specific heat curve in the temperature range of the observed reactions and the integral of an assumed straight line baseline which connects the start and end temperatures of the reactions.

As shown in Fig. 1, the dehydration thermal region occurred at temperatures of  $100 \text{ }^\circ\text{C}$  due to the release of hygroscopic moisture. Complete removal of the hygroscopic moisture under the applied unsteady state heating conditions was achieved for temperatures of up to  $150 \text{ }^\circ\text{C}$ .

The second region occurred at temperatures between  $260$  and  $425 \text{ }^\circ\text{C}$  due to decomposition of the hydroxyl bonds in the iron oxyhydroxides and release of the bound moisture. Goethite IO1 sample exhibited the most pronounced endothermic reaction in this range with a peak at

**Fig. 1** Apparent specific heat of iron ore during heating at  $10 \text{ }^\circ\text{C min}^{-1}$ ; **a** IO1; **b** IO2; **c** IO3; **d** IO4; **e** IO5

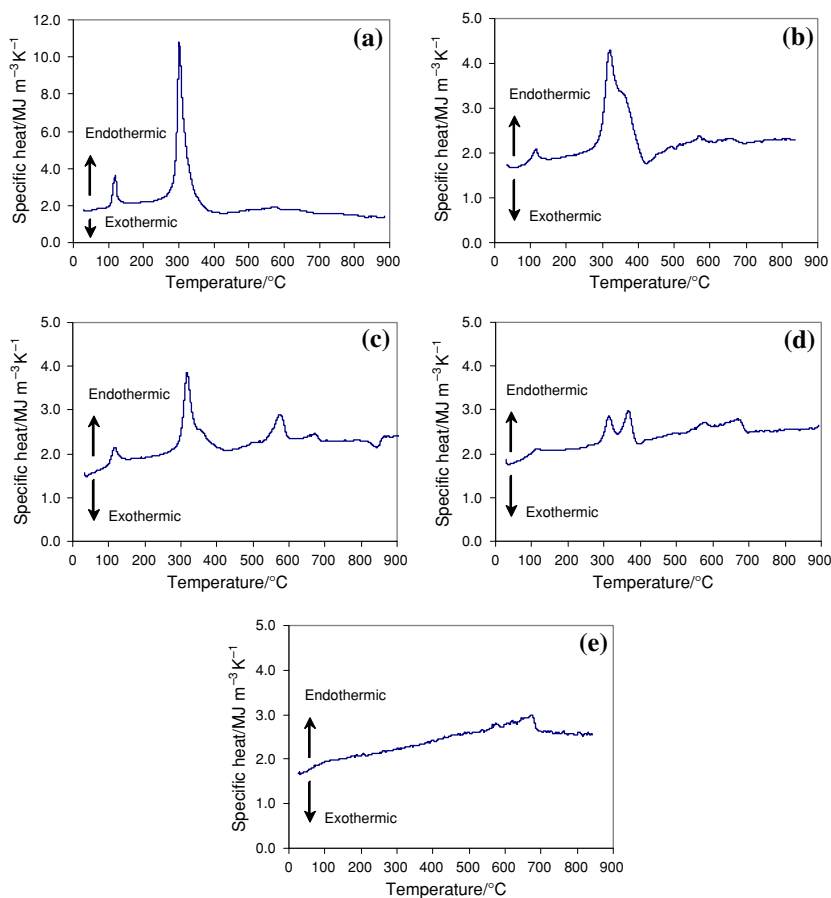
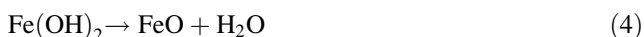
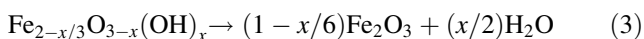
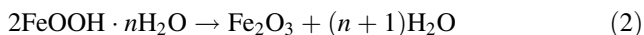


**Table 2** Iron ore mass loss/wt% and corresponding heats of reactions  $\Delta H_v/\text{MJ m}^{-3}$  for individual thermal regions

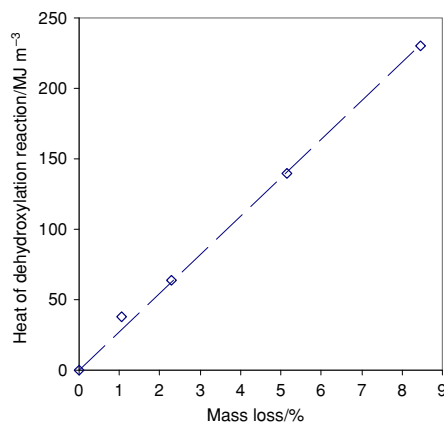
		IO1	IO2	IO3	IO4	IO5
Dehydration	Temperature range (°C)	105–150	100–130	100–150	100–130	110–125
	Mass loss wt%	0.85	0.2	0.15	<0.1	<0.1
	$\Delta H_v$ MJ m <sup>-3</sup>	21	2.8	7	1.1	0.15
Dehydroxylation	Temperature range (°C)	260–380	275–420	280–425	280–395	-
	Mass loss wt%	8.45	5.15	2.3	1.02	-
	$\Delta H_v$ MJ m <sup>-3</sup>	230	140	64	38	0
Decomposition of clays	Temperature range (°C)	540–595	555–600	530–605	555–600	550–590
	Mass loss wt%	0.95	0.7	0.95	0.45	0.3
	$\Delta H_v$ MJ m <sup>-3</sup>	2.7	2.4	28	2.8	2.0

300 °C. The endothermic dehydroxylation reactions for IO2, IO3 and IO4 were slightly different to the previous sample. The reactions for these samples appeared at higher temperature peaking at 320 °C and, in case of IO2 and IO4, the reaction went through a second endothermic peak at 368 °C. The possible different nature of the iron oxyhydroxide's dehydroxylation reaction observed in the samples can be due to chemical and/or physical reasons. Chemically there are different types of hydroxyl iron minerals occurring in the iron ore structure, such as goethite (FeO·OH), limonite (FeOOH·*n*H<sub>2</sub>O), hydrohematite (Fe<sub>2-*x*/3</sub>O<sub>3-*x*</sub>(OH)<sub>*x*</sub>), ferrihydrates (Fe<sub>2</sub>O<sub>3</sub>·*m*FeOOH·*n*H<sub>2</sub>O), iron(II) hydroxide Fe(OH)<sub>2</sub> and bernalite Fe(OH)<sub>3</sub> [5, 13, 14]. Equations 1 to 5 show the thermal decomposition pathways for the respective mineral types.



There is also a potential for ionic substitution of the iron from the goethitic crystal lattice with other metal groups, such as aluminium, calcium or manganese. Ionic substitution of the goethitic iron has been well documented to occur in goethites from soils [15, 16] Decomposition of the different metallic hydroxide groups are shown to decompose at slightly different temperatures reflecting in different reaction temperature peak occurrences [17].

The physical differences in the iron oxyhydroxides are in crystallinity and extent of isomorphous substitution. When an iron ore particle contains goethite surrounded by dense hematite the diffusion of the formed water can be restrained inside the particle, propagating cracking, increasing particle porosity while decreasing particle strength. The hematite sample IO5 in this case did not show any reaction at this temperature range due to exclusion of hydroxides. The heat of the dehydroxylation

**Fig. 2** Relationship between the heat of dehydroxylation and corresponding mass loss

reaction in all samples was found to be proportional to the iron ore mass loss for the same temperature region. Figure 2 shows a linear relationship between the measured heat of reaction ( $\Delta H_v$ ) and mass loss  $\text{ML}_{260-425\text{ °C}}$  between 260 and 425 °C which can be expressed with Eq. 6.

$$\Delta H_v (\text{MJ m}^{-3}) = 27.34 \cdot \text{ML}_{260-425\text{ °C}} (\%) \quad (6)$$

The results shown in Table 2 reveal that the dehydroxylation reactions of iron oxyhydroxides are completed at 380 °C for the goethite sample IO1 but not until 425 °C for the goethite/hematite IO3 sample. Therefore, based on these five samples, thermogravimetric analysis of iron ores at a temperature of at least 425 °C could be applied to determine the mass lost due to decomposition of the hydroxide bonds present in the iron oxides.

The specific heat results shown in Fig. 1 also reveal an endothermic reaction at a temperature range between 530 and 605 °C and a reaction peak at 575 °C, which was most pronounced for IO3. This reaction is associated with decomposition of the clay matter, as discussed previously by McCann et al. [18]. While the heat of clay decomposition in three of the examined samples (IO1, IO2 and IO4) was very similar, the iron ore sample IO3 exhibited the

largest reaction. It is very likely that the main contributor to this reaction is decomposition of the kaolinite mineral  $\text{Al}_2\text{Si}_2\text{O}_5(\text{OH})_4$  in a reaction assumed by Eq. 7. This is indicated by the largest amount of associated  $\text{Al}_2\text{O}_3$  content (see Table 1) in sample IO3.



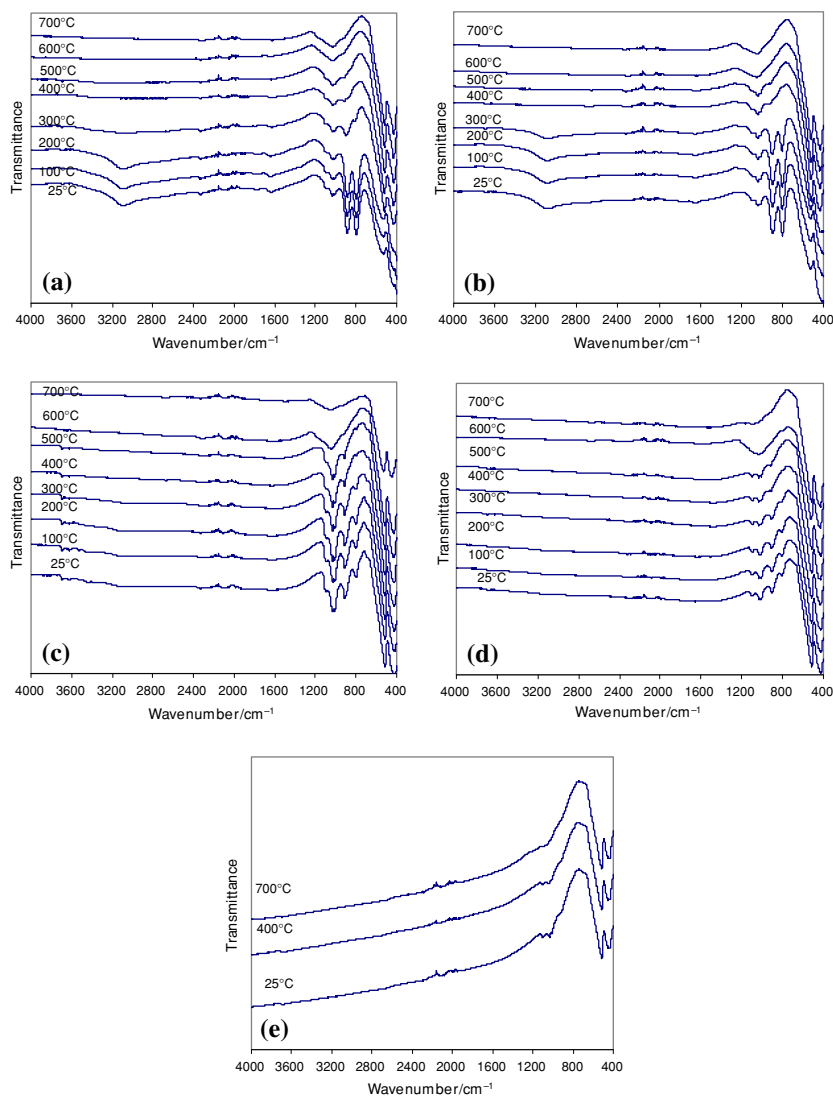
All samples exhibited a distinctive endothermic reaction with a peak at 675 °C, which relates to the magnetic transformation (Curie point) of  $\alpha\text{-Fe}_2\text{O}_3$  [19]. The most pronounced transformation was found in the hematite IO5 sample, while the goethite sample IO1 had an almost negligible change in the specific heat in this temperature range.

The FTIR spectroscopic analysis of the iron ores prepared at temperatures of up to 700 °C with a 100 °C interval are shown in Fig. 3. The FTIR analysis was conducted to show differences in the chemical bonds and bond

dissociation in iron ores with increased temperature. Two sharp peaks at 432 and 515  $\text{cm}^{-1}$  due to hematite  $\text{Fe}_2\text{O}_3$  were apparent in all samples, but were most pronounced in the primarily hematite containing IO5 sample. Goethite iron ores IO1, IO2 and to some extent IO3, exhibited a broad band with a characteristic maximum at around 3,093  $\text{cm}^{-1}$  corresponding to stretching vibration of the OH group and bonded water, which disappeared when samples were heated to 400 °C.

The FTIR results also revealed two different goethite groups. The first group contained samples IO1 and IO2 which had peaks at 800 and 890  $\text{cm}^{-1}$  corresponding to O=Fe–O–H vibrations. These peaks disappeared after heating at 400 °C when the new band appeared at around 910  $\text{cm}^{-1}$ . The latter is possibly due to the overlapping hydroxyl deformation band assigned to  $\delta'(\text{OH})$  and  $\gamma'(\text{OH})$  modes [20], which disappeared after heating at 600 °C. The second group of investigated iron ore goethite samples

**Fig. 3** FT-IR spectra of iron ores under different temperatures; **a** IO1; **b** IO2; **c** IO3; **d** IO4; **e** IO5



consisted of IO3 and IO4 samples. They showed presence of very small amount of water and OH groups during the characteristic absorption broad bands between 3,100 and 3,800  $\text{cm}^{-1}$ . The peak at 800  $\text{cm}^{-1}$ , similar to the previous group of samples, was due to the O=Fe–O–H vibrations, disappearing at 400 °C, however the second peak was at a slightly higher wavenumber of 910  $\text{cm}^{-1}$  due to the hydroxyl deformation band, which disappeared at 600 °C.

Few sharp bands were also detected in the range between 3,400–3,700  $\text{cm}^{-1}$  and noticeable three bands between 1,000 and 1,100  $\text{cm}^{-1}$  in all four goethite samples which are most pronounced for sample IO3. These peaks are found to correspond to the aluminosilicate clay minerals with monoclinic or triclinic crystal structure, such as kaolinite [21], halloysite and greenalite, which are present in the iron ores. In the larger wavelength range, four sharp peaks were noticed at 3446, 3523, 3620, 3647 and 3695  $\text{cm}^{-1}$  due to OH groups and bonded water associated with these clay minerals. When IO3 was heated to 400 °C the peaks that remained at this wavelength range were at 3,620 and 3,695  $\text{cm}^{-1}$ ; these were not present at 600 °C. In the lower wavelength range the peaks assigned to the clays were detected at 1010, 1033 and 1093  $\text{cm}^{-1}$ . All these peaks disappeared at a temperature of 600 °C leaving a single peak at 1,050–1,100  $\text{cm}^{-1}$  related to the asymmetric stretch of the Si–O–Al framework [22].

From the thermal and FTIR results it can be summarised that the dehydroxylation reactions which occur at a temperature range between 260 and 425 °C occur as a result of breaking of OH bonds and strongly bonded water, detected by the FTIR analysis in the range of 800, 890, 3093, 3446, 3523 and 3,647  $\text{cm}^{-1}$ . These bonds are assigned to, primarily, the iron oxide hydroxides and smaller amount possibly due to breaking of the bonded water in the aluminosilicate clay minerals. The clay fraction of the iron ores decomposed with an endothermic reaction at a temperature range of 530 and 600 °C during which the bonds detected at 910, 1010, 1033, 1093, 3620 and 3693  $\text{cm}^{-1}$  broke. These bonds are associated with the OH groups in the clay aluminosilicate minerals.

## Conclusions

Five different iron ores were subjected to computer aided thermal analysis and FTIR spectroscopy to determine thermal properties and assessment of bond breaking associated with the evolution of the iron ore matter termed as Loss on Ignition (LOI). The first region, at a temperature range between 100 and 150 °C, was due to dehydration of hygroscopic moisture. The results showed that it is likely the standard iron ore drying method to 110 °C slightly underestimates the strongly bonded water fraction present in the

iron ores by, in this case, up to 0.85% of the iron ore mass. Extending the iron ore drying process to 150 °C can ensure the strongly bonded hydrated compounds are fully released.

The second region of evolution of LOI matter occurred at a temperature range between 260 and 425 °C and was termed as dehydroxylation range. In this temperature region, the hydroxyl groups of various types of iron oxyhydroxides present in the iron ores are fractured. The sample mass loss in this temperature range is in linear relationship with the measured heats of reactions determined with the computational calorimetric method. The work shows that the amount of released LOI matter due to dehydroxylation may be determined with TG methods by heating the iron ore samples to temperatures slightly above 425 °C, however wider range of iron ore types may need to be tested prior to confirming this temperature is uniform for all iron ore types.

The third region of iron ore LOI matter release was related to decomposition of the OH groups in the clay materials and occurred between 530 and 605 °C. The FTIR spectra revealed that the clays composed primarily of aluminosilicate minerals with monoclinic or triclinic crystal structure, such as kaolinite, halloysite and greenalite. The magnetic transformation of  $\alpha\text{-Fe}_2\text{O}_3$  was visible in the thermal analysis data through a distinctive endothermic reaction peaking at 675 °C.

**Acknowledgements** The authors acknowledge financial support from the Australian Research Council and Hamersley Iron (grant no: LP0882722).

## References

1. Fenton MD. U.S. Geological Survey, Mineral Commodity Summaries, January 2009 [http://minerals.usgs.gov/minerals/pubs/commodity/iron\\_&\\_steel/mcs-2009-feste.pdf](http://minerals.usgs.gov/minerals/pubs/commodity/iron_&_steel/mcs-2009-feste.pdf). 2009.
2. Varajão CAC, Bruand A, Ramanaidou ER, Gilkes RJ. Microporosity of BIF hosted massive hematite ore, Iron Quadrangle, Brazil. *An Acad Bras Ciênc.* 2002;74:113–26.
3. Kim JR, Kang HS, Lee HJ, Je JH, Jeong SK, Tsai W-L, et al. Real-time microradiology of disintegration of iron ore sinteres. *Nucl Instrum Methods Phys Res B.* 2003;199:441–5.
4. Weissenborn PK, Dunn JG, Warren LJ. Quantitative thermogravimetric analysis of hematite, goethite and kaolinite in Western-Australian iron-ores. *Thermochim Acta.* 1994;239:147–56.
5. Mitov I, Paneva D, Kunev B. Comparative study of the thermal decomposition of iron oxyhydroxides. *Thermochim Acta.* 2002;386:179–88.
6. Fan H, Song B, Li Q. Thermal behavior of goethite during transformation to hematite. *Mater Chem Phys.* 2006;98:148–53.
7. O'Connor F, Cheung WH, Valix M. Reduction roasting of limonite ores: effect of dehydroxylation International. *Int J Miner Process.* 2006;80:88–99.
8. Prasad PSR, Prasad KS, Chaitanya VK, Babu EVSSK, Sreedhar B, Murthy SR. In situ FTIR study on the dehydration of natural goethite. *J Asian Earth Sci.* 2006;27:503–11.
9. Walter D. Characterization of synthetic hydrous hematite pigments. *Thermochim Acta.* 2006;445:195–9.



10. Dweck J. Qualitative and quantitative characterization of Brazilian natural and organophilic clays by thermal analysis. *J Therm Anal Calorim.* 2008;92:129–35.
11. López FA, Ramirez MC, Pons JA, López-Delgado A, Alguacil FJ. Kinetic study of the thermal decomposition of low-grade nickeliferous laterite ores. *J Therm Anal Calorim.* 2008;94:517–22.
12. Strezov V, Lucas JA, Strezov L. Computer aided thermal analysis. *J Therm Anal Calorim.* 2003;72:907–18.
13. Wolska E. The structure of hydrohematite. *Z Kristallogr.* 1981; 154:69–75.
14. Cornell RM, Schwertmann U. The iron oxides—Structure, properties, reactions, occurrences and uses. VCH: Weinheim; 2003.
15. Schulze DG. The influence of aluminum on iron oxides; VII, Unit-cell dimensions of Al-substituted goethites and estimation of Al from them. *Clays Clay Min.* 1984;32:36–44.
16. Alvarez M, Rueda EH, Sileo EE. Simultaneous incorporation of Mn and Al in the goethite structure. *Geochim Cosmochim Acta.* 2007;71:1009–20.
17. Wells MA, Fitzpatrick RW, Gilkes RJ. Thermal and mineral properties of Al- Cr- Mn- Ni- and Ti-substituted goethite. *Clays Clay Min.* 2006;54:176–94.
18. McCann G, Strezov V, Lucas J, Evans T, Strezov L. Iron ore characterisation during high temperature thermal processing. *Dev Chem Eng Min Proc.* 2004;12:369–82.
19. Lanza R, Meloni A. The Earth's magnetism. An introduction for geologists. Springer-Verlag, Berlin; 2006. p. 92.
20. Ruan HD, Frost RL, Klopogge JT. The behavior of hydroxyl units of synthetic goethite and its dehydroxylated product hematite. *Spectrochim Acta A.* 2001;57:2575–86.
21. Kristóf J, Frost RL, Felinger A, Mink J. FTIR spectroscopic study of intercalated kaolinite. *J Mol Struct.* 1997;410–411:119–22.
22. Castaldi P, Silveti M, Santona L, Enzo S, Melis P. *Clays Clay Min.* 2008;56:461–9.